Model Systems for Dissolution of Finely Divided (Multisized) Drug Powders

J. MAUGER ˣ and S. HOWARD

Abstract □ Several reports have dealt with model systems for the dissolution of log-normally distributed powders. A numerical solution is presented for the previously published Higuchi–Hiestand equations for a log-normal particle-size distribution. This solution was realized *via* an application of the System 360 Continuous System Modeling Program (CSMP). The resulting computer-aided calculations were utilized in the comparisons between the Higuchi–Hiestand model and other existing models. These comparisons provided a basis for the development of an adaptation of the Nielsen moving sphere model for log-normally distributed powders. The adaptation of the Nielsen equation for multisized particle systems is suggested as being potentially useful for treating experimental data where hydrodynamic effects must be considered.

Keyphrases □ Dissolution—model system, multisized drug powders, compared to other models □ Powders, multisized—model system for dissolution, compared to other models □ Particle-size distribution—numerical solution, multisized drug powders, model system for dissolution

Diffusional models for the description of the dissolution rate of a multisize particle population have been discussed previously (1–3). Higuchi and Hiestand (1) derived equations describing the dissolution rate of finely divided (multisized) particles in a diffusion-controlled dissolution process. The Higuchi–Hiestand treatment considered a limiting case, which is valid when hydrodynamic effects on the solute diffusion near the particles are minimal; *i.e.*, the treatment is valid for small particles. To integrate the complex equations, an approximation was assumed for a log-normal particle distribution.

In a later paper (4), the previously derived theoretical considerations were used to analyze data for the dissolution rate of a methylprednisolone suspension in water. The agreement of theory with the experimental data was reasonable in view of the fact that the theoretical values were calculated independently of the experimentally determined data.

Later papers (2, 3) noted that the original theoretical exposition of Higuchi and Hiestand had considered an approximate function for a log-normal distribution to reduce the complexity of the equations and to allow an analytical solution. Carstensen and Musa proposed a need for an analytical solution using the actual log-normal distribution rather than an approximation and accomplished the integration using numerical analysis techniques aided by a computer (2). Subsequent work (3) provided an exact treatment for the equations used by Carstensen and Musa (2).

These studies (2, 3) differed significantly from the original theoretical considerations (1). In particular, the distribution functions used for an analytical solution were different, one being an approximation and the other the actual function. In addition, an even more fundamental difference existed. Higuchi and Hiestand used a mathematical model that considered major assumptions surrounding a realistic diffusion-controlled case. But Carstensen and Musa (2) and Brooke (3) chose to use the Hixson–Crowell treatment as a basis for their analytical solutions. Although the Hixson–Crowell treatment has been tested under controlled experimental conditions for monosized particles (5), application of this model to multisized particles has not been experimentally justified. Furthermore, the Hixson–Crowell treatment anticipates significant hydrodynamic effects, and one is presumably dealing with large particles relative to those valid for use of the Higuchi–Hiestand model.

A further consideration of the differences between the Higuchi–Hiestand treatment and the Hixson–Crowell treatment centers about the diffusion layer. While the diffusion layer thickness is always the same for all particles of the same size and is comparable to or greater than the particle radius for the former, the latter ignores the effective diffusion layer or assumes that it is constant for all particles and remains constant throughout a particle's lifetime. The assumption that the effective diffusion layer is constant for all particles is particularly rigid for a multisized particle population, and the constancy throughout a particle's lifetime for any given particle has been questioned (5).

THEORY

With the limitations of the Hixson–Crowell treatment in mind, the Higuchi–Hiestand model provides a more rigorous approach but does not incorporate a quantitative consideration of the hydrodynamic effects. The Nielsen model (6) for a moving sphere is purposeful in this connection. The kinetic expression for the Nielsen model is:

$$-\frac{da}{dt} = \frac{DCF}{a(\rho_d)} \qquad \text{(Eq. 1)}$$

where a is the particle radius (centimeters), t is time (seconds), D is the diffusion coefficient (square centimeters per second), C is the saturation concentration (grams per milliliter), ρ_d is the particle density (grams per milliliter), $F = (1 + A)^{0.285}$, and A is given by:

$$A = \frac{2a^3G(\rho_d - \rho_m)}{9D\eta} \qquad \text{(Eq. 2)}$$

where $G = 981$ cm/sec^2, ρ_m is the density of the medium, and η is the viscosity of the medium (grams per centimeter per second).

The Nielsen model, as expressed by Eq. 1, considers a combined diffusion–convection-controlled dissolution rate of a particle. The model assumes that: (*a*) the dissolution rate of the particle is diffusion controlled and that convection is also contributing to the transport process, (*b*) the effective diffusion layer thickness is the same for all particles of the same size and is equal to or greater than the particle radius, (*c*) the particle is dissolving under sink conditions, and (*d*) the dissolving particle is spherical. As noted by Higuchi and Hiestand (1), the second assumption is important because it implies a quasi-steady-state condition in the diffusion layer.

The quantity A (Eq. 2) is derived from a theoretical consideration of the convection effect of a sphere moving through a liquid at a rate in keeping with Stokes' law. As the particle radius approaches zero, the quantity A also approaches zero and the parameter F in Eq. 1 approaches unity. Therefore, as F approaches unity, the Nielsen model relaxes to a pure diffusional model, *i.e.*, the Higuchi–Hiestand

Table I—Predicted Dissolution Profile for a Single Methylprednisolone Particle

Seconds	Higuchi–Hiestand Model Particle Radius, μm	Nielsen Model Particle Radius, μm
0	10.00	10.00
400	8.32	7.89
830	6.01	5.06
970	5.04	3.80

model, $-da/dt = DC/a\rho_d$. Nielsen noted that Eq. 2 is valid when the Reynolds number is less than one; under this constraint, the model becomes useful for pharmaceutical powders.

The authors applied Eq. 1 to a multisized powder population based on numbers. An expression for the weight fraction undissolved, W_f, at time t is:

$$W_f = \frac{\int_{a_{0t}}^{a_{l0}} \frac{4}{3}\pi\rho_d a_t^3 f(a_0)\, da_0}{\int_{a_{s0}}^{a_{l0}} \frac{4}{3}\pi\rho_d a_0^3 f(a_0)\, da_0} \qquad \text{(Eq. 3)}$$

The quantity $f(a_0)$ given in both the numerator and denominator of Eq. 3 is the density function for a specific number distribution of powders, with the particle radius as the random variable. The full quantity in the denominator of Eq. 3 expresses the fraction of total weight in a powder population at time zero. Therefore, integrating this quantity between the limits of the smallest particle radius at time zero, a_{s0}, and the largest particle radius of the powder at time zero, a_{l0}, gives the total weight at time zero.

The full quantity in the numerator of Eq. 3 expresses the fraction of the total weight in a powder population at time t, where a_t is the particle radius at time t and is found using either the Nielsen or Higuchi–Hiestand model *via* Eq. 1. The lower limit of integration in the numerator of Eq. 3 is the zero time radius of the particle that just dissolved, a_{0t}, and the upper limit remains set at a_{l0}. Integrating the numerator at time t yields the total weight of the powder population remaining at time t. Therefore, W_f in Eq. 3 represents the weight *fraction* undissolved at time t. The actual expressions associated with $f(a_0)$ are shown in Eqs. 4 and 5, where the approximation for the log-normal case as used by Higuchi and Hiestand is given by Eq. 4 and the approximation for the log-normal case is given by Eq. 5:

$$f(a_0) = \alpha \frac{1}{a_0^4} \qquad \text{(Eq. 4)}$$

$$f(\ln a_0) = \alpha \exp\left[-(\ln a_0 - \ln \bar{a}_0)^2/(2SDEV^2)\right] \qquad \text{(Eq. 5)}$$

where $\bar{a}_0$ in Eq. 5 is the mean of a log-normal population. Strictly speaking, the use of the log-normal case requires the integration limits in Eq. 3 to be changed to ln ( ) and $f(a_0)\, da_0$ becomes $f(\ln a_0)\, d \ln a_0$. Normalization constants associated with Eqs. 4 and 5 are not shown since they cancel to unity when $f(a_0)$ or $f(\ln a_0)$ is inserted into Eq. 3.

The purpose of this study was to use computer-generated data to compare the characteristics of the Nielsen moving sphere model with the Higuchi–Hiestand model for both mono- and multisized powder systems. These simulated data dissolution profiles should provide information concerning the use and limitations of the kinetic model as described by Eq. 1.

COMPUTATIONAL DETAILS

All solutions to Eqs. 1 and 3 were numerically obtained using System 360 Continuous System Modeling Program[1] (CSMP). Although CSMP is designed to handle time-variant problems, its usefulness is not limited to kinetic models where the limits of integration are typically zero to time t or zero to time infinity. The limits can be set to accommodate statistical populations where the limits are determined by the population under study, in this case, a particle-size population.

Table II—Predicted Dissolution Profile for a Single Methylprednisolone Particle

Seconds	Higuchi–Hiestand Model Particle Radius, μm	Nielsen Model Particle Radius, μm
0	25.0	25.0
2000	21.7	17.1
3100	19.7	12.4
4800	16.0	00.0
6100	12.5	00.0

Table III—Summary of Zero-Time Methylprednisolone Radii

Seconds	Higuchi–Hiestand Model Particle Radius, μm	Nielsen Model Particle Radius, μm
400	5.6	5.6
1500	10.7	11.6
3000	15.2	18.0
4500*	18.6	23.8

For the log-normal powder populations in the present experiment, the limits of integration were set initially to include ±10 standard deviation units, *SDEV*, of ln a_0. As the temporal behavior of a log-normal powder population is followed, the initial limits up to some critical time are $\int_{a_{s0}}^{a_{l0}}$ and later, when a_{s0} dissolves, the limits become $\int_{a_{0t}}^{a_{l0}}$, where a_{0t} is defined as the zero time radius of the particle that just dissolved[2]. The quantity a_{0t} is determined from the kinetic model given in Eq. 1.

CSMP offers a variety of routines to perform the integration operation. The routine chosen and used for all calculations was the fixed step Runge–Kutta, which provided the desired stability and accuracy. The integration step size was set by dividing the ±10 standard deviation interval into 500 intervals.

RESULTS AND DISCUSSION

An immediate purpose of this study was to conduct an analysis of the Nielsen moving sphere model and the Higuchi–Hiestand model for a single particle to demonstrate quantitatively the conditions where one may expect hydrodynamic effects to be significant.

The physical–chemical data for methylprednisolone are available[3], and computer-generated particle lifetimes *via* CSMP for the hypothetical, yet realistic, methylprednisolone example are shown in Table I. These data show that the Higuchi–Hiestand treatment is not substantially different from the Nielsen treatment for a particle with a zero time radius of 10 μm.

The half-life predicted by the Higuchi–Hiestand model is approximately 970 sec, whereas the Nielsen model predicts a half-life of about 830 sec. For larger particles, the difference is more striking (Table II). For a 25-μm particle, the Higuchi–Hiestand model predicts a half-life value of 6100 sec, while the Nielsen model predicts a value of 3100 sec. In other words, the effect of convection in addition to diffusion is contributing to the dissolution of the particle as the sphere falls through the medium at a rate in keeping with Stokes' law. Later in the particle's lifetime, when the radius approaches 10 μm, the process relaxes to a diffusion-controlled case.

The data in Table III summarize the quantitative difference between the two models. Notice in particular that the Higuchi–Hiestand model predicts that a methylprednisolone particle with a zero time radius of 18.6 μm will dissolve in 4500 sec, while the Nielsen model predicts that a methylprednisolone particle with a zero time radius of 23.8 μm will dissolve in the same time frame. Although the radius of the larger particle is only 1.28 times greater than that of the smaller, the weight of the larger particle is more than two times that of the smaller.

This single-particle example shows under what particle-size conditions one might expect the Nielsen model to be useful. In addition, the dynamic features of the Nielsen model are exemplified since the convection portion of the process will decay as the particle size diminishes.

For multisized powder populations, CSMP was used to solve nu-

[1] The system is discussed in IBM Application Program Manual 360 A-CX-16X.

[2] For the Higuchi–Hiestand model, $a_{0t} = [2DCt/\rho_d]^{1/2}$.

[3] Data were taken from Ref. 1. Saturation concentration, C, is 1.0×10^{-4} g/ml; diffusion coefficient, D, is 5.0×10^{-6} cm²/sec; and particle density, ρ_d, is 1.3 g/ml.

Table IV—Validation of the CSMP Program

Seconds	Weight Fraction Undissolved	
	CSMP	Closed Form
13	0.726	0.725
52	0.435	0.434
130	0.255	0.254
400	0.743×10^{-1}	0.741×10^{-1}

merically for the weight fraction remaining for the Higuchi–Hiestand or Nielsen moving sphere model with either the approximate log-normal or log-normal case. The program was validated by comparing the CSMP output for a multisized population against the closed form solution using the Higuchi–Hiestand model and the approximate log-normal case. The data used to generate the values in Table IV were for methylprednisolone particles where a_{s0} = 1 μm and a_{l0} = 10 μm.

The accuracy of the CSMP-generated data was consistently on the order of 0.2%. The consistency of the error is important, and these data show that the numerical process does not drift as a function of time. Other validation steps were taken and smaller programs were written to ensure the accuracy of the output.

The first log-normal population, by numbers, that was tested was assigned population parameters such that the geometric mean radius was 3.16 μm and the smallest and largest radii in the population were 1 and 10 μm, respectively. Again, methylprednisolone was used as an example of a pharmaceutical powder.

The weight fraction remaining *versus* time profile for this example is shown in Fig. 1. Note that W_f reaches zero in about 250 sec, although a methylprednisolone particle with an initial radius of 10 μm has a theoretical lifetime of 1300 sec. This finding has important experimental implications, because one cannot expect to assay the small weight that will dissolve between 250 and 1300 sec. The fact that the Nielsen model is superimposed on the Higuchi–Hiestand model is not surprising in view of the similarity of the data for the single methylprednisolone particle studies where the zero time radius equals 10 μm.

The second log-normal population studied was assigned the following population parameters: $\ln \bar{a}_0 = 2.7607$ and $SDEV = 0.04582$. Therefore, the quantity $\bar{a}_0$ corresponded to a radius of 15.8 μm, and the largest and smallest radii in the population were 25 and 10 μm, respectively. The dissolution profile for this methylprednisolone powder population (Fig. 2) shows that the particles are large enough to be sensitive to hydrodynamic effects. The W_f values for the Nielsen model are consistently smaller than those for the Higuchi–Hiestand model. This population was designed so that about 99% of the weight was within ±3 *SD* of the mean. Therefore, the standard deviation was small when compared to the mean, and approximately 75% of the total weight dissolved before the smallest particle dissolved.

The third log-normal methylprednisolone population studied was assigned the following population parameters: $\ln \bar{a}_0 = 2.7607$ and $SDEV = 0.12$. Therefore, the quantity $\bar{a}_0$ corresponded to a radius of 15.8 μm, and the largest and smallest radii in the population were

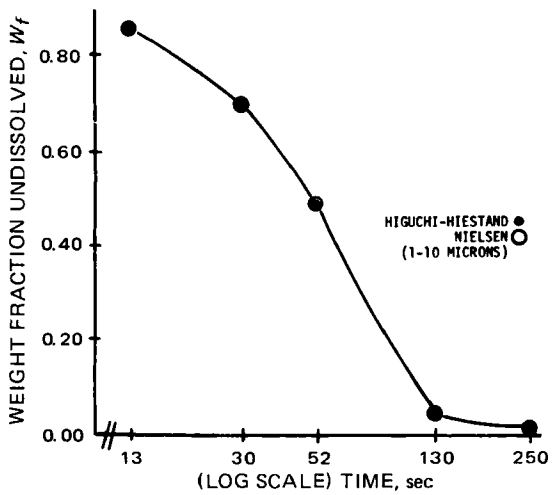

Figure 1—*Weight fraction remaining* versus *time profile.*

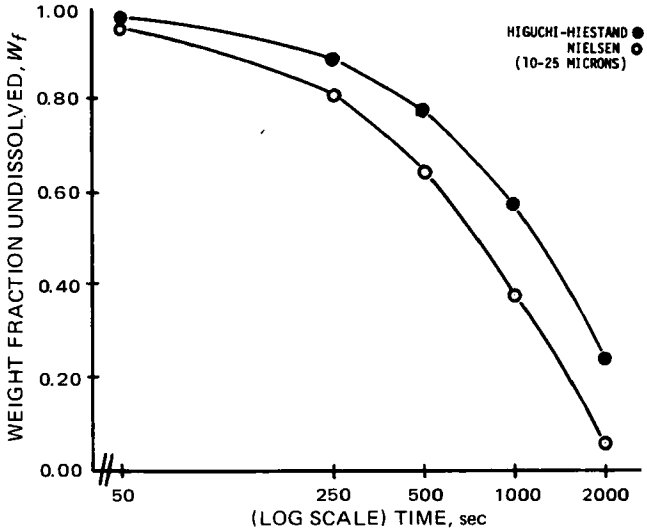

Figure 2—*Weight fraction remaining* versus *time profile.*

53 and 4.8 μm, respectively. The dissolution profile for this population is shown in Fig. 3 and is interesting because the population includes particles large enough to be very sensitive to hydrodynamic effects and particles small enough to be relatively insensitive to hydrodynamic effects. In other words, early in the dissolution profile, the large particles dissolve according to a model where both convection and diffusion are important. Later, the smaller particles have melted away and the larger particles reach a particle radius where the diffusion process predominates.

The results of this study confirm these expectations. At 500 sec, W_f for the Higuchi–Hiestand model is about 0.80; for the Nielsen model, it is 0.66. The difference between the models increases with time; at 2000 sec, W_f is 0.28 for the Higuchi–Hiestand model and 0.08 for the Nielsen model. The relative magnitude of difference between the two models shows the importance of the convection effect.

An interesting characteristic of this kinetic treatment is related to the difference between the particle and medium densities. According to Eq. 2, the difference between these two quantities is one determinant of the magnitude of *A*. Therefore, the kinetic model relies on a suspended particle population where the influence of gravity mimics stirring conditions. One might question this model when it is applied to experimental data. Experimental data are required to test this issue, but the discussion by Calderbank (7) is instructive. Calderbank argued that: "When the particles in a mixing vessel are just completely suspended, turbulence forces balance those due to gravity, and the mass-transfer rates are the same as for particles moving freely under gravity."

Calderbank also provided equations that could be used in place of

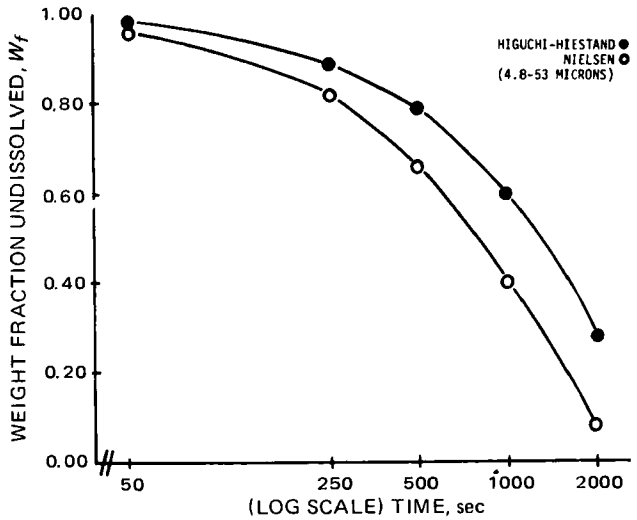

Figure 3—*Weight fraction remaining* versus *time profile.*

Stokes' law in the derivation of Eq. 2 and that account for the total shear stress which has to be generated in a mixing vessel to cause free suspension of particles. The derivation given by Goyan (8) for the Dankwerts model under laminar flow conditions of stirring relies on a physical model of a particle falling slowly in a liquid medium.

In summary, the multisized particle dissolution profiles point to actual experimental conditions where one may be dealing with a particle-size distribution broad enough to include large particles where $F > 1$ and small particles where $F = 1$. In these circumstances, a simple diffusion model would be inadequate and the Nielsen model in combination with the appropriate distribution function should more successfully predict the dissolution profile.

REFERENCES

(1) W. Higuchi and E. Hiestand, *J. Pharm. Sci.*, **52**, 67(1963).

(2) J. Carstensen and M. Musa, *ibid.*, **61**, 223(1972).

(3) D. Brooke, *ibid.*, **62**, 795(1973).

(4) W. Higuchi, E. Rowe, and E. Hiestand, *ibid.*, **52**, 162(1963).

(5) P. Niebergall, G. Milosovich, and J. Goyan, *ibid.*, **52**, 236(1963).

(6) A. Nielsen, *J. Phys. Chem.*, **65**, 46(1961).

(7) P. H. Calderbank, in "Mixing–Theory and Practice," vol. 2, V. Uhl and J. Gray, Eds., Academic, New York, N.Y., 1967, p. 2.

(8) J. E. Goyan, *J. Pharm. Sci.*, **54**, 645(1965).

ACKNOWLEDGMENTS AND ADDRESSES

Received March 10, 1975, from the *School of Pharmacy, West Virginia University, Morgantown, WV 26506*

Accepted for publication September 29, 1975.

Presented at the Basic Pharmaceutics Section, APhA Academy of Pharmaceutical Sciences, New Orleans meeting, November 1974.

[x] To whom inquiries should be directed.

Correlation of *In Vitro* and *In Vivo* Methodology for Evaluation of Antacids

R. D. SMYTH [x], T. HERCZEG, T. A. WHEATLEY, W. HAUSE, and N. H. REAVEY-CANTWELL

Abstract □ The rate and extent of acid consumption of an antacid suspension and tablet were evaluated by *in vitro* and *in vivo* techniques. Four different test procedures were used to estimate *in vitro* antacid reactivity. *In vivo* effects were determined in the fasted and postcibal states in normal human subjects by a radiotelemetry procedure. The duration of elevation of intragastric pH >3 was in agreement with *in vitro* estimates of total acid consumption of the antacid. There was also good correlation between onset, extent, and duration of *in vivo* antacid activity and a modified *in vitro* Beekman antacid test procedure. There was no significant difference in antacid activity of the tablet or suspension in either *in vitro* or *in vivo* test procedures. A wide variation in antacid activity was observed between subjects and also in the fasted *versus* postcibal states. These studies emphasize the requirements for standardization of antacid products by comparative *in vitro* and *in vivo* evaluations to facilitate individualized dose titration of the antacid in each patient and correlation of the acid secretion rate in various types of GI disease with the antacid dose.

Keyphrases □ Antacids—suspensions and tablets, rate and extent of acid consumption, *in vitro* and *in vivo* evaluations compared □ Acid consumption—rate and extent by antacid suspensions and tablets, *in vitro* and *in vivo* evaluations compared

The Food and Drug Administration (FDA) recently introduced an *in vitro* test (1) to determine the acid-neutralizing rate and acid-consuming capacity of over-the-counter antacid products. FDA also recommended that research be initiated to develop an *in vivo* model to assess antacid activity. Although an *in vitro* test can approximate *in vivo* conditions with respect to acid-consuming capacity, speed and duration of action, and maximum buffering capacity of the antacid, it cannot account for variations in antacid activity due to gastric emptying, changes in the acid secretion rate as seen in the fasting and postcibal states, interaction of antacids with glycoproteins and mucoproteins of gastric juice, coating of the gastric mucosa by antacids, and the effect of antacids on endogenous control of gastric acid secretion (2, 3).

The purpose of the present study was to compare the activity of an antacid tablet and suspension in both *in vitro* and *in vivo* models. Onset of action, maximum buffering capacity, and duration of antacid effect were compared in various *in vitro* systems and in normal human subjects in both the fasting and postcibal states.

EXPERIMENTAL

Methods—Each antacid tablet or 5 ml of suspension contained 200 mg of magnesium hydroxide, 225 mg of aluminum hydroxide, and 250 mg of calcium carbonate. The minimum recommended dose is two tablets (chewed) or 10 ml of suspension.

Total acid-consuming capacity was determined by the USP XVIII procedure (4) and by the OTC antacid test (1). A completely automated Bachrach procedure (5) was developed to determine the rate and extent of acid consumption.

A modified Beekman procedure (6, 7) was developed to determine the onset, duration, and buffering capacity of the antacid and to correlate *in vivo* and *in vitro* results. The modifications were as follows: antacid was added to 50 ml of 0.1 *N* hydrochloric acid at 37.5 ± 1° contained in a jacketed glass vessel provided with a combination pH electrode, agitator, and tubing to introduce the acid and to remove the antacid–acid mixture. The agitator was a paddle-type propeller[1] operated at approximately 400 rpm. Acid was continuously added, and the antacid–acid mixture was continuously removed at the rate of 270 ± 14 ml/hr with a positive displacement tubing pump. A glass reservoir of 0.1 *N* hydrochloric acid was maintained at 37.5 ± 1°. The pH was measured with a combination electrode and standardized pH meter connected to a recorder operating at a chart speed of 20.3 cm (8 in.)/hr.

The timer was activated, on addition of the test sample, and the pH values were recorded. The pump was then automatically started, adding 0.1 *N* hydrochloric acid and removing the antacid–acid reac-

[1] Coated with Teflon (du Pont).